https://doi.org/10.5194/hess-2021-98
Preprint. Discussion started: 8 April 2021

Hydrology and Earth System Sciences
Open Access
Discussions

In-stream *Escherichia Coli* Modeling Using high-temporal-resolution data with deep learning and process-based models

Ather Abbas[1], Sangsoo Baek[1], Norbert Silvera[2], Bounsamay Soulileuth[3], Yakov Pachepsky[4] Olivier Ribolzi[5], Laurie Boithias[5†], Kyung Hwa Cho[1†]

[1] School of Urban and Environmental Engineering, Ulsan National Institute of Science and Technology, Ulsan 689-798, Republic of Korea

[2] Institute of Ecology and Environmental Sciences of Paris (iEES-Paris), Sorbonne Université, Univ Paris Est Creteil, IRD, CNRS, INRA, Paris, France

[3] IRD, IEES-Paris UMR 242, c/o National Agriculture and Forestry Research Institute, Vientiane, Lao PDR

[4] Environmental Microbial and Food Safety Laboratory, USDA-ARS, Beltsville, MD, USA

[5] Géosciences Environnement Toulouse, Université de Toulouse, CNRS, IRD, UPS, Toulouse, France

[†] *Co-corresponding authors: Kyung Hwa Cho (khcho@unist.ac.kr), Laurie Boithias (laurie.boithias@get.omp.eu)*

https://doi.org/10.5194/hess-2021-98
Preprint. Discussion started: 8 April 2021

Abstract

Contamination of surface waters through microbiological pollutants is a major concern to public health. Although long-term and high-frequency *E. coli* monitoring can help prevent diseases from fecal pathogenic microorganisms, this monitoring is time consuming and expensive. Process-driven models are an alternative method for determining fecal pathogenic microorganisms. However, process-based modeling still has limitations in improving the model accuracy because of the complex mechanistic relationships among hydrological and environmental variables. On the other hand, with the rise in data availability and computation power, the use of data-driven models is increasing. Therefore, in this study, we simulated the transport of *Escherichia coli* (*E. coli*) in a 0.6 km² tropical headwater catchment located in Lao PDR using a deep learning model and a process-based model. The deep learning model was built using the long short-term memory (LSTM) technique, whereas the process-based model was constructed using the Hydrological Simulation Program–FORTRAN (HSPF). First, we calibrated both models for surface as well as for subsurface flow. Then, we simulated the *E. coli* transport with 6 min time steps with both the HSPF and LSTM models. The LSTM provided accurate results for surface and subsurface flow, by showing 0.51 and 0.64 of Nash–Sutcliffe Efficiency (NSE), respectively, whereas the NSE values yielded by the HSPF were -0.7 and 0.59 for surface and subsurface flow. The simulated *E. coli* concentration from LSTM also improved, yielding an NSE of 0.35, whereas the HSPF showed an unacceptable performance, with an NSE value of -3.01. This is because of the limitation of HSPF in capturing the dynamics of *E. coli* with land-use change. The simulated *E. coli* concentration showed rise and drop patterns corresponding to annual changes in land use. This study shows the application of deep learning-based models as an efficient alternative to process-based models for *E. coil* fate and transport simulation at the catchment scale.

https://doi.org/10.5194/hess-2021-98
Preprint. Discussion started: 8 April 2021

Hydrology and Earth System Sciences Discussions

Keywords: hydrological modeling; neural networks; fecal contamination; tropical rivers; South-East Asia; hydrograph separation

1 Introduction

Contamination of surface waters through microbiological pollutants is a major public health concern (Bain et al., 2014). Worldwide, pathogens have a propensity to wreak havoc on human health because of the diseases they cause, such as diarrhea, resulting in infant mortality. In particular, developing countries are vulnerable to pathogen-related diseases due to the deficit of sanitation facilities (Boithias et al., 2016). *Escherichia coli* (*E. coli*) has been frequently used as an indicator of fecal bacteria because it is easy to culture and less dangerous than other pathogens (Rochelle-Newall et al., 2015). Higher concentrations of *E. coli* in water tend to be linked to fecal pathogenic microorganisms, which are harmful to human health. Although long-term and high-frequency *E. coli* monitoring can help prevent waterborne diseases from fecal pathogenic microorganisms, the monitoring of *E. coli* concentration is time consuming and expensive (Cho et al., 2016; Frolich et al., 2017; Kim et al., 2017). High-frequency datasets of *E. coli* concentration are scarce, and available long-term datasets are often inadequate to yield a continuous concentration of fecal pathogenic microorganisms (van der Leeuw, 2004). This drawback in monitoring can be overcome by modeling approaches. Thus, they can be an alternative to determinin the fate and transport of fecal pathogenic microorganisms at the catchment scale by simulating *E. coli* in each one of the environmental compartments, for example the soil surface and streams (Ligaray et al., 2016; Perez-Pedini et al., 2005; Pacehpsky et al., 2011).

Several process-based models have been developed to model stream water contamination by *E. coli*. Popular models to simulate *E. coli* are the Soil and Water Assessment Tool (SWAT) (Neitsch et al., 2011), Hydrological Simulation Program–FORTRAN (HSPF) (Bicknell et al., 1997), INCA-pathogen (Whitehead et al., 2016), and Pathogen Catchment Budget (PCB) (Ferguson et al., 2007). The fate and transport of *E. coli* is a complex phenomenon that depends on several drivers (Pachepsky et al., 2018), such as the hydrological regime (Boithias et al., 2016; Pachepsky et al., 2017), relative contributions of both surface runoff and subsurface flow to the overall in-stream discharge (Boithias et al., 2021), concentration and sources of suspended sediment (Ribolzi et al., 2016; Nguyen et al., 2016), land use (Causse et al., 2015; Nakhle et al., 2021), intrinsic properties of the bacterium (Pachepsky et al., 2014), and economic conditions (Iqbal et al., 2019). However, the process-based model still has limitations in terms of high accuracy due to complex mechanistic relationships among hydrological and environmental variables (Abimbola et al., 2020). In addition, the simplified equations of these models might increase the inherent uncertainties, resulting in simulation errors. The *E. coli* concentration in surface water varies significantly within a very short span of time (Chen et al., 2014; Boithias et al., 2021). Daily and weekly simulations cannot capture the dynamics of *E. coli* in a short duration. In particular, the simulation with high-resolution frequency is important in small headwater catchments because the duration of flood events might be less than one day (Gassman et al., 2007). Therefore, an *E. coli* concentration simulation with high-frequency resolution should be conducted to determine the temporal distribution of *E. coli*.

Recently, deep learning (DL) has become a promising alternative approach for estimating water quality by using features of water constituent dynamics (Pyo et al., 2021). Long short-term memory (LSTM) networks have an advantage over other deep learning-based models in that they can extract complex patterns from sequence data (Schmidthuber and Hochreiter, 1997). Several studies have applied deep learning to water quality modeling and prediction (Peterson et al., 2020; Isikdogan et al., 2017; Solanki et al., 2015). Dong et al. (2019) used LSTM to predict dissolved oxygen and showed that LSTM performs better than machine learning methods, such as autoregressive integrated moving average or artificial neural networks. Although LSTM has been used extensively for building hydrological models (Abbas et al., 2020), its potential has not yet been explored to estimate *E. coli* concentration in stream waters. Deep learning-based models have also not been developed for the simulation of water quality with high-resolution frequency.

This study aims to evaluate the applicability of LSTM to simulate in-stream *E. coli* concentration with high temporal resolution. In addition, the process-based model HSPF was used as a benchmark to compare and assess the performance of LSTM. Both models were applied in a 0.6 km² tropical headwater catchment from the northern Lao People's Democratic Republic (PDR). The temporal resolution of the simulations was 6 min in both models. Thus, the specific objectives of this study were to compare the performance of a process-based model and a deep learning model 1) to simulate both surface and subsurface flow, 2) to simulate *E. coli* concentration, and 3) to analyze the response of *E. coli* by changing land use.

https://doi.org/10.5194/hess-2021-98
Preprint. Discussion started: 8 April 2021

2 Materials and Methods

2.1 Study site and data acquisition

The study area is the Houay Pano headwater catchment, located 10 km south of the city of Luang Prabang, Lao PDR (Boithias et al., 2021) (Fig. 1). This catchment is representative of a montane agroecosystem in Southeast Asia and is part of the long-term critical zone observatories' network called multiscale TROPIcal CatchmentS (M-TROPICS), which is affiliated with the French research infrastructure OZCAR (Gaillardet et al., 2018). This site had undergone rapid land-use changes from 2011 to 2018 (Fig. S1a). The characteristics of this area, including land use information, are provided in the supplementary information (Text S1). We collected climate, hydrological, *E. coli* concentration, and electrical conductivity data at 6 min time steps from 2011 to 2018. Rainfall, relative humidity, solar radiation, wind speed, and air temperature were measured with an automatic weather station Campbell Scientific BWS200, which was equipped with ARG100 (a 0.2 mm capacity tipping bucket). The potential evapotranspiration was calculated using the Penman–Monteith method. We measured the stream water level at the monitoring station using a V-notch and water-level recorder (OTT Thalimedes). The discharge was estimated based on the rating curve between the discharge and water levels. The surface and subsurface flow were calculated using the electrical conductivity method (Ribolzi et al., 2018). A detailed description of this method is provided in the supplementary information (Text S2). *E. coli* concentration was measured based on the standardized microplate method (ISO 9308–3). A detailed explanation of *the E. coli* experiment can be found in the supplementary information (Text S3). In this study, we carried out biweekly grab sampling of *E. coli* from 2011 to 2018. Over the same period, we also specifically sampled 11 flood events to assess *E. coli* dynamics during flood events by using an

https://doi.org/10.5194/hess-2021-98
Preprint. Discussion started: 8 April 2021

automated sampler (ICRISAT) triggered by the water level recorder to collect water after every 2 cm water level change during flood rising and every 5 cm water level change during flood recession. The total number of *E. coli* samples collected over the 2011–2018 period was 255. In addition, we collected the monthly number of poultries, swine, goats, and the number of humans who visited the study area. These data were used to quantify the source of *E. coli* in this catchment (Rochelle-Newall et al., 2016) (Fig. S1b).

2.2 Flow and *E. coli* concentration simulation.

In this study, HSPF and LSTM models were used to simulate in-stream surface flow, subsurface flow, and *E. coli* concentration. HSPF and LSTM are popular models among the process-based and DL models (Bicknell et al., 1997; Ahmadisharaf and Benham, 2020; Kratzert et al., 2019). Both models have been adopted for hydrological and water quality simulations (Peterson et al., 2020; Isikdogan et al., 2017; Ahmed et al., 2014). In the HSPF, the simulation of surface and subsurface flow and of *E. coli* concentration was carried out in three steps: (1) building the model, (2) conducting sensitivity analysis based on the Latin-Hypercube–One-factor-At-a-Time (LH-OAT), and 3) calibrating the model using the Newton algorithm (Nash, 1984). A schematic of the LSTM simulation is shown in Fig. 2. The first step in building this model was data preparation (Fig. 2a). LSTM then simulated surface and subsurface flow with climate data (Fig. 2b). Finally, we estimated the *E. coli* concentration at 6 min intervals using rainfall, bacteria source, land-use change, and surface and subsurface flow (Fig. 2c). Both models considered the source of *E. coli* to simulate its concentration at the catchment outlet. The fecal matter from the *E. coli* sources was assumed to be evenly distributed in the catchment. The monthly *E. coli* source

https://doi.org/10.5194/hess-2021-98
Preprint. Discussion started: 8 April 2021

data is presented in Fig. S1b. The time series data of the *E. coli* source was used as input for the *E. coil* simulation.

https://doi.org/10.5194/hess-2021-98
Preprint. Discussion started: 8 April 2021

2.2.1 Hydrological Simulation Program Fortran (HSPF)

The HPSF model is a process-driven model that simulates processes at the catchment scale (Bicknell et al., 1997). It has been extensively used to model the fate and transport of *E. coli* in catchments (Ahmadisharaf and Benham, 2020; Chin et al., 2009) and to develop total maximum daily loads of *E. coli* at various locations (Mishra et al. 2018; Yagow et al., 1998). The original software was written in the FORTRAN programming language. Recently, the Hydrological Simulation Program Python (HSP2) was developed based on the Python programming language (van Rossum, 2007). HSP2 is a platform-independent software that extends the functionality of HSPF by allowing the use of dynamic variables and easier management of input and output files (Heaphy et al., 2015). The HSPF simulates the hydrological cycle by discretizing the catchment into pervious and impervious hydrological response units (HRUs). Previous HRUs simulate evapotranspiration, surface detention, surface infiltration, interflow, baseflow, and deep percolation, whereas impervious HRUs simulate surface detention and surface flow (Bicknell et al., 1997). The simulation of in-stream *E. coli* concentration in HSPF is based on a first-order kinetics approach, considering the decay rate (Fonseca et al., 2014). Detailed descriptions of hydrological and *E. coli* simulations can be found in Bicknell et al. (1997). For this study, we rewrote the modules of *E. coli* simulation, and the simulation was carried out in the Python programming language. This allowed us to incorporate more dynamic use of input data, such as the annual change in land use and the monthly bacterial source.

In our study, HRUs were divided into four units based on land use: Forest, Fallow, Teak, and Annual crop. Among land uses, we did not consider any imperviousness in the Forest and Fallow. We considered 2 % and 1 % imperviousness for the Teak and Annual crop land uses (Patin

https://doi.org/10.5194/hess-2021-98
Preprint. Discussion started: 8 April 2021

et al., 2018). We selected 13 and 4 parameters for each land use for the sensitivity analysis of hydrological and *E. coil* simulations, respectively (Table 1 and Table S1). The total number of parameters for hydrological and *E. coil* simulation were 52 and 18, respectively. In model calibration, we selected the 25 most sensitive parameters of the hydrological simulation and all parameters of the *E. coli* simulation. Sensitivity analysis and model calibration were conducted based on the LH-OAT and the Newton algorithm, respectively. A detailed explanation of the LH-OAT and the Newton algorithm can be found in the Supplementary Information (Text S4).

2.2.2 Long short-term memory (LSTM)

In the data preparation step (Fig. 2a), our data were converted to a 6 min frequency. We then built the LSTM model to simulate surface and subsurface flow using the validated model structure (Abbas et al., 2020) (Fig. 2b). It uses historical data of rainfall, solar radiation, air temperature, and potential evapotranspiration to simulate surface and subsurface flow. To simulate the output at a time-step “t,” LSTM uses the data of previous “n” time steps as inputs (Chollet, 2018). The inputs from previous time steps are used by LSTM to predict the output at the next time step (t+1). The number of these time steps “n” are called lookback steps (Chollet, 2018). The simulated surface and subsurface flow from the LSTM were applied to simulate the *E. coli* concentration (Fig. 2c). We adopted a bacterial source and land-use information as input for the LSTM. To investigate the impact of land-use change on in-stream *E. coli* concentration, we conducted *E. coli* simulations in two scenarios. In scenario 1, we used the land-use change and *E. coli* source information separately. In scenario 2, we calculated the *E. coli* source per area for each land use.

LSTM is a special type of recurrent neural network designed to extract temporal features from sequence data (Hochreiter and Schmidhuber, 1997). An LSTM cell is the basic building block of the LSTM (Fig. S2). It consists of three “gates” and two “states” The gates are “forget,” “update,” and “output,” which decide what information to forget, allow in, and allow out from the LSTM “memory,” respectively. The states act as a memory or information carrier across time. The equations describing the functions of gates and states are as follows:

$$C_c^{<t>} = tanh(W_c[\, h^{<t-1>}, x^{<t>}] + \, b_c), \tag{1}$$

$$\Gamma_f = \sigma(W_f[c^{<t-1>}, x^{<t>}] + b_{f)}, \tag{2}$$

$$\Gamma_o = \sigma(W_o[c^{<t-1>}, x^{<t>}] + b_{o)}, \tag{3}$$

$$\Gamma_u = \sigma(W_u[c^{<t-1>}, x^{<t>}] + b_{u)}, \tag{4}$$

$$C^{<t>} = \Gamma_u * C_c^{<t>} + \Gamma_f * C^{<t-1>} \tag{5}$$

$$h^{<t>} = \Gamma_o * tanh\, C^{<t>}. \tag{6}$$

The symbol $*$ in the above equations represents elementwise multiplication. The behavior of each gate is controlled by the weights (W) and biases (b) associated with them. Their output was further modified by a nonlinear function (σ). At each time step (t), the prospective cell state ($C_c^{<t>}$) is calculated based on the output from the previous time step ($h^{<t-1>}$) and the input from the current time step ($x^{<t>}$) (Eq. 1). The notation $W_c[h^{<t-1>}, x^{<t>}]$ represents pointwise multiplication of new inputs and previous hidden state with the weight matrix W_c separately and then adding their output. This prospective cell state ($C_c^{<t>}$), along with the output from the "forget" and "update" gate decides the current cell state ($c^{<t>}$) (Eq. 5). The current cell state and output gate control the output values from LSTM ($h^{<t>}$), the so-called hidden state (Eq. 6). The hyperbolic tangent ($tanh$) is another nonlinearity used in LSTM for the calculation of the cell state (Eq. 1) and the output state (Eq. 6). Equations 1–6 are used to calculate the LSTM output, which is then compared with observed values to calculate the error. This study used the mean square error (MSE) as the error function.

We used the TensorFlow software v1.15 for building the LSTM model (Abadi et al., 2016). We used an Intel® Core™ i7-9700 processor with a graphics card of NVIDIA GeForce RTX 2080 having 12 GB of dedicated GPU memory, along with 64 GB of Random-Access Memory for simulating surface, subsurface, and *E. coli*.

https://doi.org/10.5194/hess-2021-98
Preprint. Discussion started: 8 April 2021

Hydrology and Earth System Sciences Discussions Open Access EGU

2.2.3 Hyperparameters of LSTM

The structure and performance of the LSTM were controlled by hyperparameters, including the dropout rate, LSTM units, learning rate, lookback steps, and activation functions for both LSTM and the fully connected layer (Table 2). Dropout is a regularization technique that switches off a certain number of nodes in the LSTM (Goodfellow et al., 2016). This simple technique helps break the brittle coadaptation of weights, which hinders generalization to unseen data. This way, dropout prevents overfitting (Srivastava et al., 2014). In overfitting, the model performs better on calibration data, but its performance deteriorates on new unseen data. The number of LSTM units directly corresponds to the learning capacity of LSTM, but it also accounts for more memory and computation. This number determines the size of the weight matrix of an LSTM. The learning rate defines the change in the weights of the neural network during calibration (Goodfellow et al., 2016). A higher number of lookback steps allows LSTM to capture long-term patterns at the cost of an increase in memory consumption and computation. The activation function determines the nonlinearity in the model.

2.3 Performance statistics

Evaluations to assess the performance of the HSPF and LSTM were conducted using MSE, Nash–Sutcliffe efficiency (NSE), and percent bias (PBIAS) (Nash and Sutcliffe, 1970; Gupta et al., 1999). NSE is useful for interpreting the model performance by generating a dimensionless value as the performance index (Lin et al., 2017). The PBIAS measures the average tendency of the simulated data to be overestimated or underestimated than observed

https://doi.org/10.5194/hess-2021-98
Preprint. Discussion started: 8 April 2021

Hydrology and Earth System Sciences
Open Access
EGU
Discussions

values (Moriasi 2007). The MSE, NSE, and PBIAS were calculated using the following equations:

$$MSE = \frac{\left[\sum_{i=1}^{n}(o_i - p_i)^2\right]}{n} \tag{7}$$

$$\mathrm{NSE} = 1 - \frac{\sum(o_i - p_i)^2}{\sum(o_i - \bar{o})^2} \tag{8}$$

$$\mathrm{PBIAS} = 1 - \frac{\sum_{i=1}^{n} o_i - p_i}{\sum_{i=1}^{n} o_i} \tag{9}$$

where p_i is the simulated data, o_i is the observed data, and n is the number of points in the data.

https://doi.org/10.5194/hess-2021-98
Preprint. Discussion started: 8 April 2021

3 Results and discussion

3.1 Land use change and *E. coli* source

The land-use change from 2011 to 2018 is shown in Fig. S1a. The area of Fallow land-use increased from 2011 to 2016, whereas Annual crop area decreased. Teak tree plantations were expanded until 2013 and were retained. Forest land use accounted for about 10 % of the study area from 2011 to 2018. In general, the land-use change has been dynamic from 2011 to 2013, whereas its variation diminished from 2016 to 2018. Previous studies have demonstrated that the expansion of Teak trees might increase the surface flow (Ribolzi et al., 2017; Song et al., 2020). Higher runoff at the soil surface may cause a higher inflow of *E. coli* with surface flow. The monthly *E. coli* source in the catchment decreased from 2×10^{15} in 2011 to 3×10^{14} in 2018 (Fig. S1b). This decrease in *E. coli* source is caused by the decrease in manpower needed in Teak tree plantations and in Fallow plots, compared to the Annual crop (Fig. S1a) (Boithias et al., 2021).

https://doi.org/10.5194/hess-2021-98
Preprint. Discussion started: 8 April 2021

3.2 Sensitivity analysis and optimization result

The sensitivity results for the flow simulation are shown in Fig. S3, and the most sensitive parameters are listed in Table S2. The interflow and infiltration-related parameters were the most sensitive parameters for surface and subsurface flows. The Manning's "n" value (NSUR) for Teak and Fallow land uses was among the 10 most sensitive parameters. Kim et al. (2017) suggested that Manning's value is the most sensitive parameter in the hydrological simulation of tropical headwater catchments, such as the Houay Pano catchment in northern Lao PDR. The groundwater recession rate (AGWRC) and soil infiltration capacity (INFILD) were sensitive to subsurface flow. In Annual crop land use, infiltration capacity (INFILT) and upper zone storage (UZSN) were the most sensitive parameters. Abbas et al. (2020) demonstrated that INFILT is the most sensitive parameter for subsurface flow in tropical subcatchments.

The sensitivity analysis results for *E. coli* are shown in Fig. S4 and Table S3. The parameters related to the transport of *E. coli* on the land surface (e.g., WSQOP, SQOLIM_MF) were more sensitive than other parameters. IOQC and AOQC were the least sensitive parameters. These parameters are related to *E. coli* transport in interflow and baseflow (Bicknell et al., 2011). This implies that the in-stream *E. coli* concentration at the study site is mainly driven by surface flow (Boithias et al., 2021). A previous study also demonstrated that 89 % of in-stream *E. coli* concentrations were driven by surface flow (Boithias et al., 2021). Figure 3 shows the model performance dependent on different objective functions. We found that the model performance was better when the NSE was selected as the objective function. The NSE of the surface and subsurface flow was positive by optimizing with NSE. However, the NSE value for surface flow

https://doi.org/10.5194/hess-2021-98
Preprint. Discussion started: 8 April 2021

Hydrology and Earth System Sciences
Discussions
Open Access

was negative when the objective function was MSE during the optimization. Negative NSE indicated an "unsatisfactory" performance range (Moriasi et al., 2015).

3.3 Flow simulation

The simulated surface and subsurface flow using the HSPF are plotted in Fig. 4. We found that the simulated subsurface flow was underestimated compared to the observations. Although surface flow from the HSPF followed the trend and peaks of observations, this model yielded a negative NSE value, indicating that the model simulation was unacceptable (Moriasi et al., 2015) (Table 3). The NSE values for subsurface flow from HSPF were 0.49 and 0.59 for calibration and validation, respectively. Hence, the HSPF model is better at simulating subsurface flow than surface flow. In particular, the simulated surface flow was underestimated compared to the observations. The average values of INFILT and UZSN were 0.36 and 1.22, respectively, which were larger than those reported in previous studies (Lee et al., 2020). INIFILT controls the overall division of available moisture into the surface and subsurface (Bicknell et al., 2001). The parameter UZSN influences the evapotranspiration process (Bicknell et al., 2001). This underestimation of surface flow using HSPF is consistent with a previous study (Kim et al., 2017). We also investigated the impact of underestimation and overestimation of the flow by plotting flow duration curves (Fig. S5). Although both flows can capture the peak flow, the simulated subsurface flow was still underestimated compared to the observed subsurface flow.

The simulated surface and subsurface flows using the LSTM model are plotted in Fig. 5. The NSE values for the calibration period were 0.56 and 0.69 for surface and subsurface flow, respectively. The corresponding validation NSE of the surface and subsurface flow were 0.51 and

https://doi.org/10.5194/hess-2021-98
Preprint. Discussion started: 8 April 2021

0.64, respectively. These results indicate that the LSTM had a satisfactory performance for both the calibration and validation periods according to the criteria of Moriasi et al. (2015). LSTM overcame the problem of the HSPF model underestimating subsurface flow. In addition, the peak surface flows from the LSTM were similar to observations. The observed and simulated flows in storm events are presented in Figs. S6–S11. LSTM can follow the observed trends in surface and subsurface flow more closely than the HSPF. This leads to increased NSE values for both surface flow as well as for subsurface flow. The hyperparameters of the LSTM are described in Table 2. The rectified linear unit (ReLU) was chosen as the activation function for the LSTM output. Because the simulated *E. coli* should be positive, we chose ReLU, which cannot produce negative values from the model (Nair and Hinton, 2010). The optimal batch size and LSTM units were 16 and 100, respectively. The optimal value of the lookback steps was 50, which is equal to 5 h of input data.

We analyzed the model performance for surface and subsurface flows during storm events (Fig. 6). These events were selected where the peak flow exceeded 0.2 m per s. The performance of LSTM is considerably better than that of HSPF for most storm events. In surface flow, the average MSE of LSTM and HSPF was 1.1e-4 and 6.1e-4 (m^3s^{-1}), respectively. The NSE values from LSTM varied from 0.2 to 0.6, whereas that of HSPF ranged from -1.0 to 0.4. We found that the NSE values from the HSPF vary considerably depending on storm events. On June 11, 2015, the NSE value of HSPF was as high as 0.4, whereas for some others it was below 0. Although the subsurface flow of the HSPF provided better model performance than surface flow simulation, this model still presented an unacceptable result with a negative NSE value.

https://doi.org/10.5194/hess-2021-98
Preprint. Discussion started: 8 April 2021

3.4 *E. coli* simulation

Figure 7 shows the temporal distribution of *E. coli* concentration using HSPF and LSTM. The *E. coli* concentration from HSPF was overestimated compared to the observed *E. coli* concentration. The performance matrices of the HSPF were also worse than those of the LSTM (Table 4**)**. In particular, the HSPF simulation presented a PBIAS value of 73, indicating an overestimation of *E. coli* concentration (Moriasi et al., 2015). Ackerman and Weisman (2014) reported that the *E. coli* simulation from HPSF was overestimated compared to observation. The overestimation of simulated *E. coli* at tropical sites has also been observed by Kim et al. (2017). *E. coli* simulation from LSTM is satisfactory in both calibration and validation periods according to the criteria set by Moriasi et al. (2015). In contrast, the HSPF result can be regarded as "unsatisfactory" in both the calibration and validation periods. These results implied that LSTM could generate acceptable performances and had good agreement between the observed and simulated *E. coli*.

The simulation during the storm events using both the HSPF and LSTM models are shown in Fig. 8 and Figs. S6–S11. Figure 8 shows the storm events from the validation data, whereas the other figures show the storm events from the calibration data. In general, the simulated *E. coli* by HPSF and LSTM were overestimated and underestimated, respectively. This difference might be caused by the fact that *E. coli* from HSPF is more responsive to surface flow, wheras *E. coli* from LSTM is more influenced by subsurface flow (Ackerman and Weisman, 2014). The sensitivity analysis of HSPF also demonstrated that the influence of interflow and baseflow on *E. coli* is weaker than surface flow because the parameters IOQC and AOQC are the least sensitive parameters for *E. coli* simulation. Both parameters affect the *E. coli* concentration in interflow and

https://doi.org/10.5194/hess-2021-98
Preprint. Discussion started: 8 April 2021

baseflow (Bicknell et al., 2001). The simulated *E. coli* of LSTM rose sharply and dropped slowly, similar to the observations, whereas that of the HSPF decreased steeply (Figures S6–S11). Although both models simulated the peak time of the *E. coil* correctly, the HSPF was limited to simulate a slope in its falling limb. This performance difference between both models was caused by the extent of influence from hydrological variables (e.g., rainfall, surface flow, and subsurface flow) to model output. LSTM was effective in reflecting the response of variables to output (Kratzert et al., 2019).

The performance matrices for the LSTM and HSPF models during storm events are shown in Fig. 9. In general, we observed better LSTM performance than HSPF for both NSE and MSE values. The HSPF model performed better than the LSTM for only two storm events on June 15, 2014, and June 11, 2015. For the remaining storm events, the NSE values from LSTM are higher than those of the HSPF—an NSE range from 0.20 to 0.65. Similarly, for MSE values, the LSTM was superior to the HSPF for all storm events except for the storm events of June 15, 2014, and June 11, 2015.

We observed the impact of logarithmic and minmax transformations on model performance (Fig. 10). The result of the logarithmic transformation was closer to the observation than the minmax transformation by showing an NSE of 0.57. A negative PBIAS value was obtained in logarithmic transformation. This indicated that the simulated *E. coli* from logarithmic transformation was underestimated, whereas the result of the minmax transformation was overestimated. The reason for this behavior can be attributed to the ability of minmax scaler to be more sensitive to outliers (Chuang et al., 2010). As a result, if a better accuracy during storm events is required, the target variable can be transformed on a logarithmic scale prior to calibration. This is because log transformation can reduce the effect of outliers from data (Singh and Kingsbury, 2017). It has been reported that log transformation can improve the performance of data-driven models when the data contain outliers (Zheng and Casari, 2018).

3.5 *E. coli* response to land-use change

We investigated the impact of land-use change and bacterial sources on the in-stream *E. coli* concentration simulation (Fig. 11). In scenario 1, we used land-use change time-series information (Fig. S2a) and bacterial source information (Fig. S2b). In scenario 2, we divided the bacterial source by the fraction of each land use (Fig. S2c). In scenario 1, we observed a larger variation in *E. coli* concentration from 2014 to 2018 (Fig. 11a), whereas in scenario 2, the variation in *E. coli* was smaller than that in scenario 1 (Fig. 11b). This variation in *E. coli* was due to land-use change in scenario 1. In particular, *E. coli* in 2016 was less than in other years because Annual crop land use decreased. On the other hand, the variation in *E. coli* was not observed in scenario 2 from 2015 to 2017. Neither scenario showed a significant response from 2011 to 2014. During these years, the rise in Fallow land use was complemented by a decrease in Annual crop land use.

https://doi.org/10.5194/hess-2021-98
Preprint. Discussion started: 8 April 2021

3.6 Limitations and future research

Transport of soil particles by surface flow and suspended sediments within the stream play a crucial role in the fate and transport of *E. coli* (Thupaki et al., 2013). Several studies have emphasized the importance of particle size (Cho et al., 2010), adsorption to soil and sediment particles (Palmateer et al., 1993), and resuspension of *E. coli* (Kim et al., 2017) with streambed sediments for modeling the fate and transport of *E. coli* at the catchment scale. In this study, we did not consider sediment transport, nor the attachment/detachment of *E. coli* on/from soil particles and suspended sediments. Several studies have been conducted on the monitoring and modeling of *E. coli* without considering sediment transport (Ahmadisharaf and Benham, 2020; Mishra et al., 2018). However, the need for its inclusion has been indicated elsewhere (Pandey and Soupir, 2013). To model sediment transport, additional data on suspended sediment concentration are required to build both the HSPF and deep learning-based models. Therefore, this modeling exercise can be further improved by collecting sediment-related data and modeling sediment transport along with *E. coli* concentration.

4 Conclusions

In this study, we simulated the transport of bacteria in a headwater catchment of the northern Lao PDR at 6 min time steps. The main findings of this study are summarized as follows:

- Both the LSTM and HSPF models can accommodate land-use change and bacteria-source variation with time.
- The performance of the surface and subsurface flow simulation of LSTM was superior for both the calibration and validation steps when compared with the HSPF. The LSTM provided accurate results for surface and subsurface flow by showing NSE values of 0.51 and 0.59, respectively, whereas the HSPF showed -0.7 and 0.55 of NSE.
- Our LSTM model showed better performance compared to HSPF for *E. coli* simulation. The NSE of the HSPF and LSTM were -3.01 and 0.35, respectively. We found that the LSTM model can respond to changes in land use.

This study shows that deep learning-based models are an efficient alternative to process-based models to simulate *E. coli* in a given catchment. Because LSTM can generate reasonable *E. coli* simulations, it could be applied to provide effective strategies for diseases that wreak havoc on human health. Therefore, a deep learning approach can be useful in developing better water sustainability and management.

https://doi.org/10.5194/hess-2021-98
Preprint. Discussion started: 8 April 2021

Hydrology and Earth System Sciences
Open Access
Discussions

Code Availability

Programming Language: Python

Software development: PyCharm

Year first available: 2021

Software Availability: contact the authors

Contact Address: School of Urban and Environmental Engineering, Ulsan National Institute of Science and Technology, UNIST-gil 50, Ulsan, 689–798, Republic of Korea. E-mail: khcho@unist.ac.kr

Author contributions

Ather Abbas: Conceptualization, Data curation, Methodology, Visualization, Writing - original draft, Writing - review & editing. **Sangsoo Baek:** Visualization, Writing - review & editing. **Olivier Ribolzi:** review & editing. **Norbert Silvera:** Data curation. **Bounsamay Soulileuth**: Sampling and data preparation. **Yakov Pachepsky:** review & editing. **Laurie Boithias:** Funding acquisition, Supervision, Validation, Writing - review & editing. **Kyung Hwa Cho:** Conceptualization, Funding acquisition, Supervision, Validation, Writing - review & editing.

Competing Interests

The authors declare that they have no conflict of interest.

Acknowledgments

This study was supported by Basic Science Research Program through the National Research Foundation of Korea (NRF) funded by the Ministry of education (No. 2017R1D1A1B04033074). The authors sincerely thank the Lao Department of Agricultural Land Management (DALaM) for its support, including granting the permission for field access, and the M-TROPICS Critical Zone Observatory (https://mtropics.obs-mip.fr/), which belongs to the French Research Infrastructure OZCAR (http://www.ozcar-ri.org/) for data access.

References

Abbas, A., Baek, S., Kim, M., Ligaray, M., Ribolzi, O., Silvera, N., ... and Cho, K. H.: Surface and sub-surface flow estimation at high temporal resolution using deep neural networks. *Journal of Hydrology*, 125370. https://doi.org/10.1016/j.jhydrol.2020.125370, 2020.

Abimbola, O. P., Mittelstet, A. R., Messer, T. L., Berry, E. D., Bartelt-Hunt, S. L., and Hansen, S. P.: Predicting Escherichia coli loads in cascading dams with machine learning: An integration of hydrometeorology, animal density and grazing pattern. *Science of The Total Environment*, 137894. https://doi.org/10.1016/j.scitotenv.2020.137894, 2020.

Abimbola, O., Mittelstet, A., Messer, T., Berry, E., and van Griensven, A.: Modeling and Prioritizing Interventions Using Pollution Hotspots for Reducing Nutrients, Atrazine and E. coli Concentrations in a Watershed. *Sustainability*, *13*(1), 103. https://doi.org/10.3390/su13010103, 2021.

Abadi, M., Barham, P., Chen, J., Chen, Z., Davis, A., Dean, J., ... and Kudlur, M.: Tensorflow: A system for large-scale machine learning. In *12th {USENIX} symposium on operating systems design and implementation ({OSDI} 16)* (pp. 265-283), 2016.

Ackerman, D., and Weisberg, S. B.: Evaluating HSPF runoff and water quality predictions at multiple time and spatial scales. *SBW a. K. Miller (Ed.), Southern California coastal water research project biennial report*, *2006*, 293-303, 2005.

https://doi.org/10.5194/hess-2021-98
Preprint. Discussion started: 8 April 2021

Adomat, Y., Orzechowski, G. H., Pelger, M., Haas, R., Bartak, R., Nagy-Kovács, Z. Á., ... and Grischek, T.: New Methods for Microbiological Monitoring at Riverbank Filtration Sites. *Water*, *12*(2), 584. https://doi.org/10.3390/w12020584, 2020.

Ahmadisharaf, E., and Benham, B. L.: Risk-based decision making to evaluate pollutant reduction scenarios. *Science of The Total Environment*, *702*, 135022. https://doi.org/10.1016/j.scitotenv.2019.135022, 2020.

Ahmed, S. I., Singh, A., Rudra, R., and Gharabaghi, B.: Comparison of CANWET and HSPF for water budget and water quality modeling in rural Ontario. *Water Quality Research Journal of Canada*, *49*(1), 53-71, 2014.

Benham, B., Yagow, G., Barham, B., Zeckoski, R., and Dillaha, T.: Total Maximum Daily Load Development: Mill Creek bacteria (E. coli) impairment, Page County, Virginia. Richmond, Va.: Virginia Department of Environmental Quality, 2005.

Bicknell, B. R., Imhoff, J. C., Kittle Jr, J. L., Donigian Jr, A. S., and Johanson, R. C.: Hydrological simulation program—FORTRAN user's manual for version 11. *Environmental Protection Agency Report No. EPA/600/R-97/080. US Environmental Protection Agency, Athens, Ga.*, 1997.

Boithias, L., Choisy, M., Souliyaseng, N., Jourdren, M., Quet, F., Buisson, Y., ... and Pierret, A.: Hydrological regime and water shortage as drivers of the seasonal incidence of diarrheal diseases in a tropical montane environment. *PLoS neglected tropical diseases*, *10*(12), e0005195. https://doi.org/10.1371/journal.pntd.0005195, 2016.

Causse, J., Billen, G., Garnier, J., Henri-des-Tureaux, T., Olasa, X., Thammahacksa, C., ... and Ribolzi, O.: Field and modelling studies of Escherichia coli loads in tropical streams of montane agro-ecosystems. *Journal of Hydro-Environment Research*, *9*(4), 496-507. https://doi.org/10.1016/j.jher.2015.03.003, 2015.

Chen, H. J., and Chang, H.: Response of discharge, TSS, and E. coli to rainfall events in urban, suburban, and rural watersheds. *Environmental Science: Processes & Impacts*, *16*(10), 2313-2324, 2014.

Chen, K., Chen, H., Zhou, C., Huang, Y., Qi, X., Shen, R., ... and Zhang, Y.: Comparative analysis of surface water quality prediction performance and identification of key water parameters using different machine learning models based on big data. *Water Research*, *171*, 115454. https://doi.org/10.1016/j.watres.2019.115454, 2020.

Chin, D. A., Sakura-Lemessy, D., Bosch, D. D., and Gay, P. A.: Watershed-scale fate and transport of bacteria. *Transactions of the ASABE*, *52*(1), 145-154. https://doi.org/10.13031/2013.25955, 2009.

Cho, K. H., Pachepsky, Y. A., Kim, J. H., Guber, A. K., Shelton, D. R., and Rowland, R.: Release of Escherichia coli from the bottom sediment in a first-order creek: Experiment and reach-specific modeling. *Journal of Hydrology*, *391*(3-4), 322-332. https://doi.org/10.1016/j.jhydrol.2010.07.033, 2010.

Cho, K. H., Pachepsky, Y. A., Oliver, D. M., Muirhead, R. W., Park, Y., Quilliam, R. S., and Shelton, D. R.:. Modeling fate and transport of fecally-derived microorganisms at the watershed scale: state of the science and future opportunities. *Water research*, *100*, 38-56. https://doi.org/10.1016/j.watres.2016.04.064, 2016.

Chuang, C. C., Wang, C. M., and Li, C. W.: Weighted linear regression for symbolic interval-values data with outliers. In *2010 5th IEEE Conference on Industrial Electronics and Applications* (pp. 2238-2242). IEEE, 2010.

Clevert, D. A., Unterthiner, T., and Hochreiter, S.: Fast and accurate deep network learning by exponential linear units (elus). *arXiv preprint arXiv:1511.07289*. 2015.

Chollet, F.: *Deep Learning mit Python und Keras: Das Praxis-Handbuch vom Entwickler der Keras-Bibliothek*. MITP-Verlags GmbH & Co. KG. 2018.

Dosovitskiy, A., and Djolonga, J.: You Only Train Once: Loss-Conditional Training of Deep Networks. In *International Conference on Learning Representations*. https://openreview.net/pdf?id=HyxY6JHKwr, September 2019.

Dong, Q., Lin, Y., Bi, J., and Yuan, H.: An Integrated Deep Neural Network Approach for Large-Scale Water Quality Time Series Prediction. In *2019 IEEE International Conference on Systems, Man and Cybernetics (SMC)* (pp. 3537-3542). IEEE, October 2019.

Frolich, L., Vaizel-Ohayon, D., and Fishbain, B.: Prediction of Bacterial Contamination Outbursts in Water Wells through Sparse Coding. *Scientific Reports*, *7*(1), 1-11. https://doi.org/10.1038/s41598-017-00830-4, 2017.

Fujioka, R. S., Solo-Gabriele, H. M., Byappanahalli, M. N., and Kirs, M. US recreational water quality criteria: a vision for the future. *International journal of environmental research and public health*, *12*(7), 7752-7776. 10.3390/ijerph120707752, 2015.

https://doi.org/10.5194/hess-2021-98
Preprint. Discussion started: 8 April 2021

Gaillardet, J., Braud, I., Hankard, F., Anquetin, S., Bour, O., Dorfliger, N., ... and Zitouna, R.: OZCAR: The French network of critical zone observatories. *Vadose Zone Journal*, *17*(1), 1-24. https://doi.org/10.2136/vzj2018.04.0067, 2018.

Gassman, P. W., M.R. Reyes, C.H. Green, J.G. Arnold.: The soil and water assessment tool: historical development, applications, and future research directions Trans. ASABE, 50 (4), pp. 1211-1250, 10.13031/2013.23637, 2007.

Goodfellow, I., Bengio, Y., and Courville, A.: *Deep learning*: MIT press, 2016.

Gupta, H. V., Sorooshian, S., and Yapo, P. O.: Status of automatic calibration for hydrologic models: Comparison with multilevel expert calibration. *Journal of hydrologic engineering*, *4*(2), 135-143. https://doi.org/10.1061/(ASCE)1084-0699(1999)4:2(135, 1999.

Gupta, H. V., Kling, H., Yilmaz, K. K., and Martinez, G. F.: Decomposition of the mean squared error and NSE performance criteria: Implications for improving hydrological modelling. *Journal of hydrology*, *377*(1-2), 80-91. https://doi.org/10.1016/j.jhydrol.2009.08.003, 2009.

Heaphy, R. T., Burke, M. P., and Love, J. T.: Conversion of HSPF Legacy Model to a Platform-Independent, Open-Source Language. *AGUFM*, *2015*, H13C-1529, 2015.

https://doi.org/10.5194/hess-2021-98
Preprint. Discussion started: 8 April 2021

Hinton, G. E., Osindero, S., and Teh, Y. W.: A fast learning algorithm for deep belief nets. *Neural computation*, *18*(7), 1527-1554. https://doi.org/10.1162/neco.2006.18.7.1527, 2006.

Iqbal, M. S., Islam, M. M., and Hofstra, N.: The impact of socio-economic development and climate change on E. coli loads and concentrations in Kabul River, Pakistan. *Science of the Total Environment*, *650*, 1935-1943. https://doi.org/10.1016/j.scitotenv.2018.09.347, 2019.

Kim, M., Boithias, L., Cho, K. H., Silvera, N., Thammahacksa, C., Latsachack, K., ... and Ribolzi, O.: Hydrological modeling of fecal indicator bacteria in a tropical mountain catchment. *Water research*, *119*, 102-113. https://doi.org/10.1016/j.watres.2017.04.038, 2017.

Kratzert, F., Klotz, D., Shalev, G., Klambauer, G., Hochreiter, S., and Nearing, G.: Towards learning universal, regional, and local hydrological behaviors via machine learning applied to large-sample datasets. *Hydrology & Earth System Sciences*, *23*(12). https://doi.org/10.5194/hess-23-5089-2019, 2019.

Lerios, J. L., and Villarica, M. V.: Pattern Extraction of Water Quality Prediction Using Machine Learning Algorithms of Water Reservoir. *International Journal of Mechanical Engineering and Robotics Research*, *8*(6), 2019.

Liu, P., Wang, J., Sangaiah, A. K., Xie, Y., and Yin, X.: Analysis and prediction of water quality using LSTM deep neural networks in IoT environment. *Sustainability*, *11*(7), 2058, 2019.

Lin, F., Chen, X., and Yao, H.: Evaluating the use of Nash-Sutcliffe efficiency coefficient in goodness-of-fit measures for daily runoff simulation with SWAT. *Journal of Hydrologic Engineering*, *22*(11), 05017023. https://doi.org/10.1061/(ASCE)HE.1943-5584.0001580, 2017.

Mazzocchi, F.: Could Big Data be the end of theory in science? A few remarks on the epistemology of data-driven science. *EMBO reports*, *16*(10), 1250-1255. https://doi.org/10.15252/embr.201541001, 2015.

Mishra, A., Ahmadisharaf, E., Benham, B. L., Wolfe, M. L., Leman, S. C., Gallagher, D. L., ... and Smith, E. P.: Generalized likelihood uncertainty estimation and Markov chain Monte Carlo simulation to prioritize TMDL pollutant allocations. *Journal of Hydrologic Engineering*, *23*(12), 05018025. https://doi.org/10919/93506, 2018.

Morris, M. D.: Factorial sampling plans for preliminary computational experiments. *Technometrics*, *33*(2), 161-174, 1991.

Nakhle, P., Ribolzi, O., Boithias, L., Rattanavong, S., Auda, Y., Sayavong, S., Zimmermann, R., Soulileuth, B., Pando, A., Thammahacksa, C., Rochelle-Newall, E., Santini, W., Martinez, J.M., Gratiot, N., Pierret, A.: Effects of hydrological regime and land use on in-stream Escherichia coli concentration in the Mekong basin, Lao PDR. Sci. Rep. In press, 2021.

Nash, J. E., and Sutcliffe, J. V.: River flow forecasting through conceptual models part I—A discussion of principles. *Journal of hydrology*, *10*(3), 282-290, 1970.

Nash, S. G. (1984). Newton-type minimization via the Lanczos method. *SIAM Journal on Numerical Analysis*, *21*(4), 770-788.

Nguyen, H. T. M., Le, Q. T. P., Garnier, J., Janeau, J. L., and Rochelle-Newall, E.: Seasonal variability of faecal indicator bacteria numbers and die-off rates in the Red River basin, North Viet Nam. *Scientific Reports*, *6*(1), 1-12. https://doi.org/10.1038/srep21644, 2016.

Odonkor, S. T., and Ampofo, J. K.: Escherichia coli as an indicator of bacteriological quality of water: an overview. *Microbiology research*, *4*(1), e2-e2. https://doi.org/10.4081/mr.2013.e2, 2013.

Muirhead, R. W., and Meenken, E. D.: Variability of Escherichia coli Concentrations in Rivers during Base-Flow Conditions in New Zealand. *Journal of environmental quality*, *47*(5), 967-973. https://doi.org/10.2134/jeq2017.11.0458, 2018.

Nair, V., and Hinton, G. E.: Rectified linear units improve restricted boltzmann machines. In *ICML*, January 2010.

Palmateer, G., McLean, D., Kutas, W. L., and Meissner, S. M.: Suspended particulate/bacterial interaction in agricultural drains. *SS RAO*, 1-40, 1993.

Pachepsky, Y. A., Blaustein, R. A., Whelan, G., and Shelton, D. R.: Comparing temperature effects on Escherichia coli, Salmonella, and Enterococcus survival in surface waters. *Letters in applied microbiology*, *59*(3), 278-283. https://doi.org/10.1111/lam.12272, 2014.

Pachepsky, Y., Stocker, M., Saldaña, M. O., and Shelton, D.: Enrichment of stream water with fecal indicator organisms during baseflow periods. *Environmental monitoring and assessment*, *189*(2), 51. https://doi.org/10.1007/s10661-016-5763-8, 2017.

Pachepsky, Y. A., Allende, A., Boithias, L., Cho, K., Jamieson, R., Hofstra, N., and Molina, M.: Microbial water quality: monitoring and modeling. *Journal of environmental quality*, *47*(5), 931-938. https://doi.org/10.2134/jeq2018.07.0277, 2018.

Pandey, P. K., and Soupir, M. L.: Assessing the impacts of E. coli laden streambed sediment on E. coli loads over a range of flows and sediment characteristics. *JAWRA Journal of the American Water Resources Association*, *49*(6), 1261-1269. https://doi.org/10.1111/jawr.12079, 2013.

Park, Y., Kim, M., Pachepsky, Y., Choi, S. H., Cho, J. G., Jeon, J., and Cho, K. H.: Development of a nowcasting system using machine learning approaches to predict fecal contamination levels at recreational beaches in Korea. *Journal of environmental quality*, *47*(5), 1094-1102. https://www.doi.org/10.2134/jeq2017.11.0425, 2018.

Pool, S., Vis, M., and Seibert, J.: Evaluating model performance: towards a non-parametric variant of the Kling-Gupta efficiency. *Hydrological Sciences Journal*, *63*(13-14), 1941-1953. 2018.

Pyo, J., Park, L. J., Pachepsky, Y., Baek, S. S., Kim, K., and Cho, K. H.: Using convolutional neural network for predicting cyanobacteria concentrations in river water. *Water Research*, *186*, 116349. https://doi.org/10.1016/j.watres.2020.116349, 2020.

Read, J. S., Jia, X., Willard, J., Appling, A. P., Zwart, J. A., Oliver, S. K., ... and Steinbach, M.: Process-guided deep learning predictions of lake water temperature. *Water Resources Research*, *55*(11), 9173-9190. https://doi.org/10.1029/2019WR024922, 2019.

Rochelle-Newall, E., Nguyen, T. M. H., Le, T. P. Q., Sengtaheuanghoung, O., and Ribolzi, O.: A short review of fecal indicator bacteria in tropical aquatic ecosystems: knowledge gaps and future directions. *Frontiers in microbiology*, *6*, 308. https://doi.org/10.3389/fmicb.2015.00308, 2015.

Ribolzi, O., Evrard, O., Huon, S., Rochelle-Newall, E., Henri-des-Tureaux, T., Silvera, N., ... and Sengtaheuanghoung, O.: Use of fallout radionuclides (7 Be, 210 Pb) to estimate resuspension of Escherichia coli from streambed sediments during floods in a tropical montane catchment. *Environmental Science and Pollution Research*, *23*(4), 3427-3435, 2016.

Rumelhart, D. E., Hinton, G. E., and Williams, R. J.: Learning representations by back-propagating errors. *nature*, *323*(6088), 533-536. https://doi.org/10.1038/323533a0, 1986.

Seong, C. H., Benham, B. L., Hall, K. M., and Kline, K.: Comparison of alternative methods to simulate bacteria concentrations with HSPF under low-flow conditions. *Applied Engineering in Agriculture*, *29*(6), 917-931. https://doi.org/10.13031/aea.29.10203, 2013.

Singh, A., and Kingsbury, N.: Dual-tree wavelet scattering network with parametric log transformation for object classification. In *2017 IEEE International Conference on Acoustics, Speech and Signal Processing (ICASSP)* (pp. 2622-2626). IEEE. 10.1109/ICASSP.2017.7952631, March 2017.

Song, L., Boithias, L., Sengtaheuanghoung, O., Oeurng, C., Valentin, C., Souksavath, B., ... and Ribolzi, O.: Understory Limits Surface Runoff and Soil Loss in Teak Tree Plantations of Northern Lao PDR. *Water*, *12*(9), 2327. https://doi.org/10.3390/w12092327, 2020.

Sowah, R. A., Bradshaw, K., Snyder, B., Spidle, D., and Molina, M.: Evaluation of the soil and water assessment tool (SWAT) for simulating E. coli concentrations at the watershed-scale. *Science of the Total Environment*, *746*, 140669. https://doi.org/10.1016/j.scitotenv.2020.140669, 2020.

Srivastava, N., Hinton, G., Krizhevsky, A., Sutskever, I., and Salakhutdinov, R.: Dropout: a simple way to prevent neural networks from overfitting. *The journal of machine learning research*, *15*(1), 1929-1958, 2014.

Thupaki, P., Phanikumar, M. S., Schwab, D. J., Nevers, M. B., and Whitman, R. L.: Evaluating the role of sediment-bacteria interactions on Escherichia coli concentrations at beaches in southern Lake Michigan. *Journal of geophysical research: oceans*, *118*(12), 7049-7065. https://doi.org/10.1002/2013JC008919, 2013.

https://doi.org/10.5194/hess-2021-98
Preprint. Discussion started: 8 April 2021

Hydrology and Earth System Sciences
Discussions

Troeger, C., Forouzanfar, M., Rao, P. C., Khalil, I., Brown, A., Reiner Jr, R. C., ... and Alemayohu, M. A.: Estimates of global, regional, and national morbidity, mortality, and aetiologies of diarrhoeal diseases: a systematic analysis for the Global Burden of Disease Study 2015. *The Lancet Infectious Diseases*, *17*(9), 909-948. doi:https://doi.org/10.1073/pnas.1109326109, 2017.

Van Rossum, G.: Python programming language. In *USENIX annual technical conference* (Vol. 41, p. 36), June 2007.

Virtanen, P., Gommers, R., Oliphant, T. E., Haberland, M., Reddy, T., Cournapeau, D., ... and van der Walt, S. J.: SciPy 1.0: fundamental algorithms for scientific computing in Python. *Nature methods*, *17*(3), 261-272. https://doi.org/10.1038/s41592-019-0686-2, 2020

Wang, X., Zhang, F., and Ding, J.: Evaluation of water quality based on a machine learning algorithm and water quality index for the Ebinur Lake Watershed, China. *Scientific reports*, *7*(1), 1-18. https://doi.org/10.1038/s41598-017-12853-y, 2017

https://doi.org/10.5194/hess-2021-98
Preprint. Discussion started: 8 April 2021

Xiang, Z., Yan, J., and Demir, I.: A rainfall-runoff model with LSTM-based sequence-to-sequence learning. *Water resources research*, *56*(1), e2019WR025326. https://doi.org/10.1029/2019WR025326, 2020.

Van der Leeuw, S. E.: Why model? *Cybernetics and Systems*, *35*(2-3), 117-128. https://doi.org/10.1080/01969720490426803, 2004.

Yagow, G., Dillaha, T., Mostaghimi, S., Brannan, K., Heatwole, C., and Wolfe, M. L.: TMDL modeling of fecal coliform bacteria with HSPF. In *2001 ASAE Annual Meeting* (p. 1). American Society of Agricultural and Biological Engineers, 1998.

Zheng, A., and Casari, A.: *Feature engineering for machine learning: principles and techniques for data scientists*. " O'Reilly Media, Inc.", 2018.

https://doi.org/10.5194/hess-2021-98
Preprint. Discussion started: 8 April 2021

Hydrology and Earth System Sciences
Discussions

Table 1: Optimal values and range of HSPF parameters for surface and sub-surface flows and *E. coli* concentration. Bold parameters were optimized during flow calibration process. All parameters related to *E. coli* were optimized during model calibration.

	Parameters	**Land use**				**Lower Limit**	**Upper Limit**
		Forest	**Teak**	**Fallow**	**Annual Crop**		
Surface and sub-surface flow	INFILT	**0.31**	**0.39**	**0.39**	**0.36**	0.001	0.5
	INFILD	2.0	**1.94**	**1.95**	**1.55**	1.0	3.0
	INTFW	2.60	**7.01**	**7.01**	5.64	1.0	10.0
	UZSN	1.36	1.47	**0.84**	**1.24**	0.05	2.0
	LZSN	**8.88**	**9.43**	**4.18**	**8.66**	2.0	10.0
	AGWETP	0.02	**0.007**	0.02	**0.06**	0.0	0.2
	NSUR	**0.18**	**0.39**	**0.15**	**0.43**	0.05	0.5
	BASETP	**0.05**	**0.09**	0.095	**0.003**	0.0	0.2
	DEEPFR	0.28	0.16	0.21	**0.20**	0.0	0.5
E. coli concentration	SQOLIM MF	4.99	1.35	2.04	0.53	0.5	10
	WSQOP	9.12	9.31	8.87	9.38	0.1	10.0
	IOQC	5367	8337	8380	8756	1000	10000
	AOQC	8672	7474	5465	8776	1000	10000
	FSTDEC	3.04				0.1	10.0
	THFST	1.92				1.01	2.0

https://doi.org/10.5194/hess-2021-98
Preprint. Discussion started: 8 April 2021

Hydrology and Earth System Sciences
Open Access
EGU
Discussions

Table 2: Hyper-parameters of LSTM for surface flow, sub-surface flow and *E. coli* concentration simulation.

Parameter	Surface and sub-surface flow	*E. coli*
Activation function (LSTM Layer)	Rectified Linear Unit (ReLU)	Rectified Linear Unit (ReLU)
Activation function (Dense Layer)	Rectified Linear Unit (ReLU)	Rectified Linear Unit (ReLU)
Batch size	128	16
Learning rate	1e-5	1e-6
lookback steps	5 hours	5 hours
Dropout	0.3	0.3
Hidden units	64	100
Input data	Rainfall, Solar Radiation, Air Temperature, Potential Evapotranspiration	Rainfall, Surface flow, Sub-surface flow, Land use, Bacteria source
Calibration epochs	500	7000
Training samples	490000	182
Test samples	210000	73

https://doi.org/10.5194/hess-2021-98
Preprint. Discussion started: 8 April 2021

Hydrology and Earth System Sciences
Discussions

746 **Table 3:** Performance metrics of HSPF and LSTM model for surface and sub-surface flow.

Model	Flow Type	Scenario	MSE (m^3s^{-1})	NSE	PBIAS
HSPF	Surface Flow	Calibration	6.4e-4	-0.02	-59
		Validation	4.7e-5	-0.7	-28
	Sub-surface Flow	Calibration	2.7e-4	0.49	-51
		Validation	5.e-4	0.59	-22
LSTM	Surface Flow	Calibration	1.4e-4	0.56	-48
		Validation	1.9e-4	0.51	-63
	Sub-surface Flow	Calibration	5.4e-3	0.69	-42
		Validation	5.9e-3	0.64	-46

747

https://doi.org/10.5194/hess-2021-98
Preprint. Discussion started: 8 April 2021

Hydrology and Earth System Sciences
Open Access
EGU
Discussions

748 **Table 4:** Performance metrics of HSPF and LSTM for *E. coli* concentration simulation.

Model	Scenario	MSE (MPN 100 mL^{-1})	NSE	PBIAS
HSPF	Calibration	$1.4e^{8}$	-0.29	-58
	Validation	$1.9e^{8}$	-3.01	73.01
LSTM	Calibration	$7.1e^{6}$	0.39	-1.49
	Validation	$3.0e^{7}$	0.35	62.72

749

https://doi.org/10.5194/hess-2021-98
Preprint. Discussion started: 8 April 2021

Hydrology and Earth System Sciences
Discussions

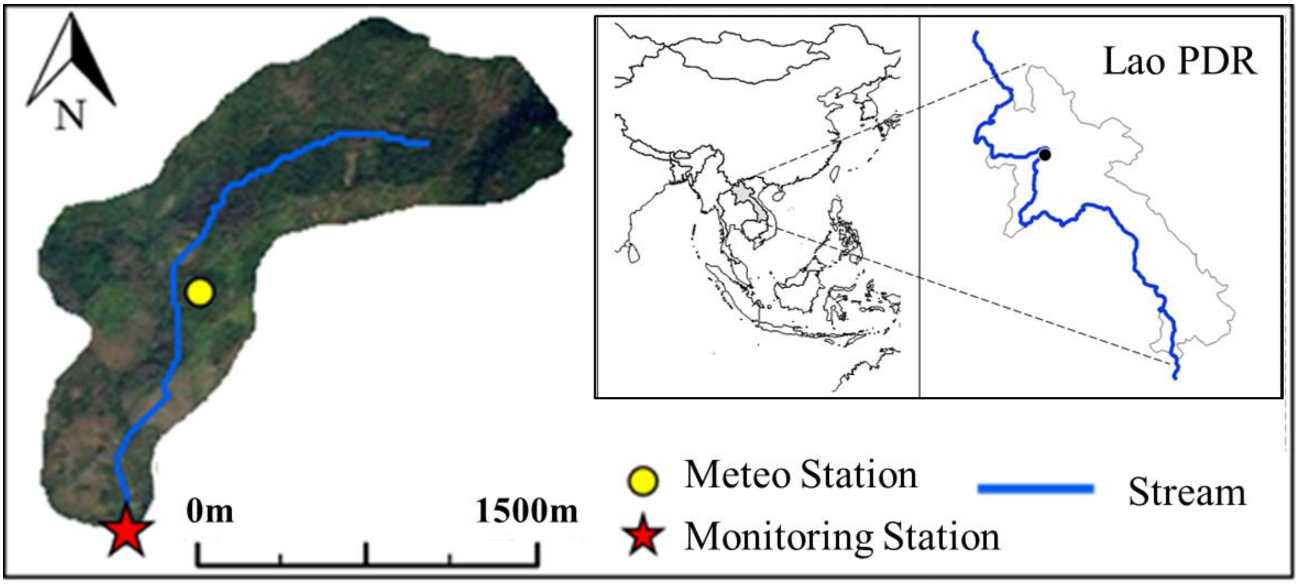

Figure 1: Location of the study area. The study area is located near Luang Prabang in northern Lao PDR. The monitoring station is located at the outlet of the catchment, where water level is recorded, and where water samples are collected for *E. coli* concentration measurement. Climate data was measured at the meteorological station.

https://doi.org/10.5194/hess-2021-98
Preprint. Discussion started: 8 April 2021

Hydrology and Earth System Sciences
Discussions

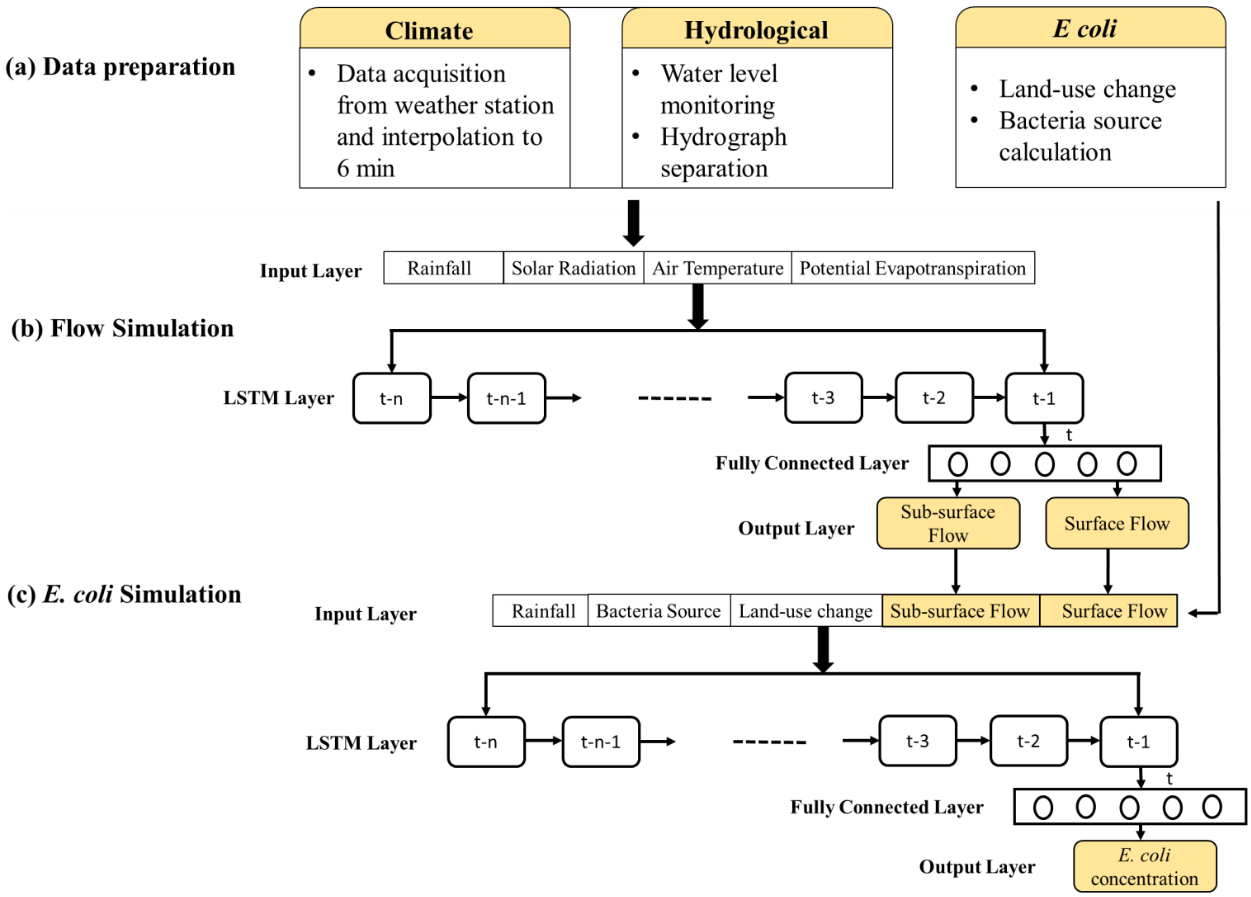

Figure 2: Structure of the LSTM Model. Environmental data is used to predict surface flow and sub-surface flow. Simulated flows along with bacteria source, land-use information and rainfall is used to simulate *E. coli* concentration. The 'n' represents the length of input data used by LSTM.

https://doi.org/10.5194/hess-2021-98
Preprint. Discussion started: 8 April 2021

Hydrology and Earth System Sciences
Discussions

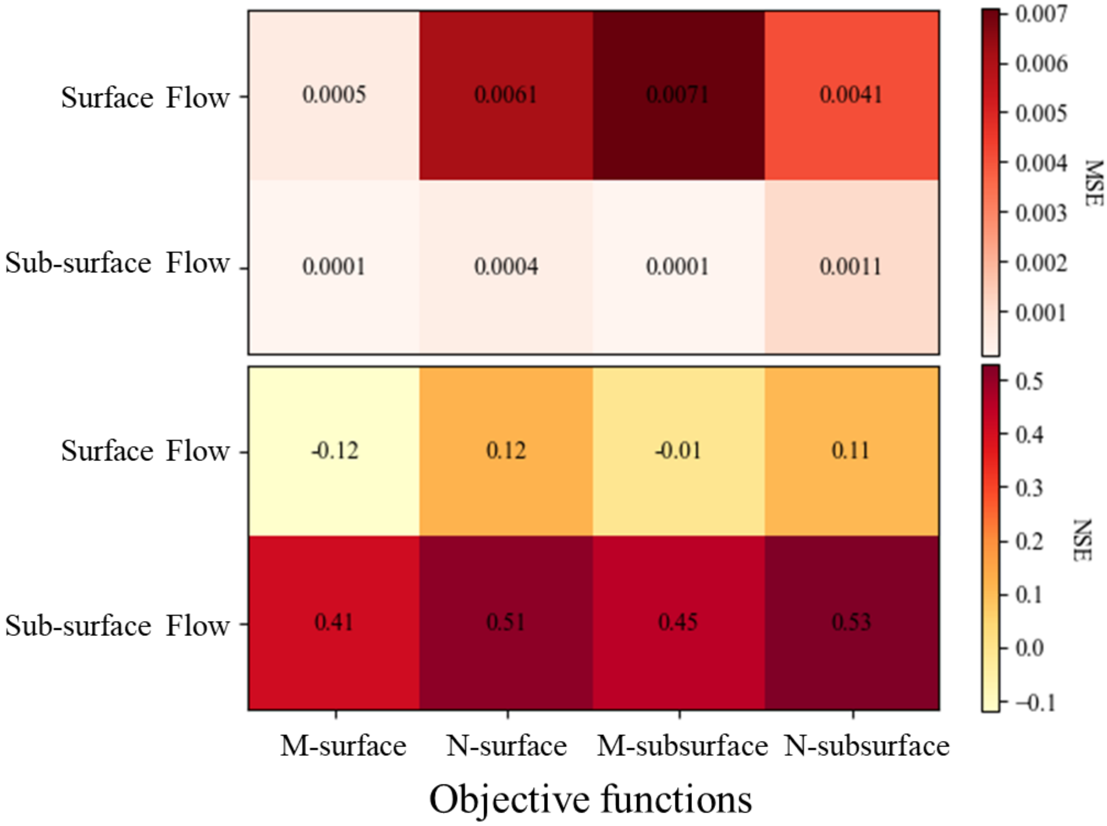

Figure 3: Performance of HSPF model with different objective functions (e.g., M-surface, N-Surface, M-subsurface and N-subsurface). The color indicates the value of MSE and NSE. M-surface is the objective function based on MSE and surface flow, N-surface is the objective function based on NSE and surface flow, M-subsurface is the objective function based on MSE and sub-surface flow, and N-subsurface is the objective function based on NSE and sub-surface flow.

https://doi.org/10.5194/hess-2021-98
Preprint. Discussion started: 8 April 2021

Hydrology and Earth System Sciences
Open Access
EGU
Discussions

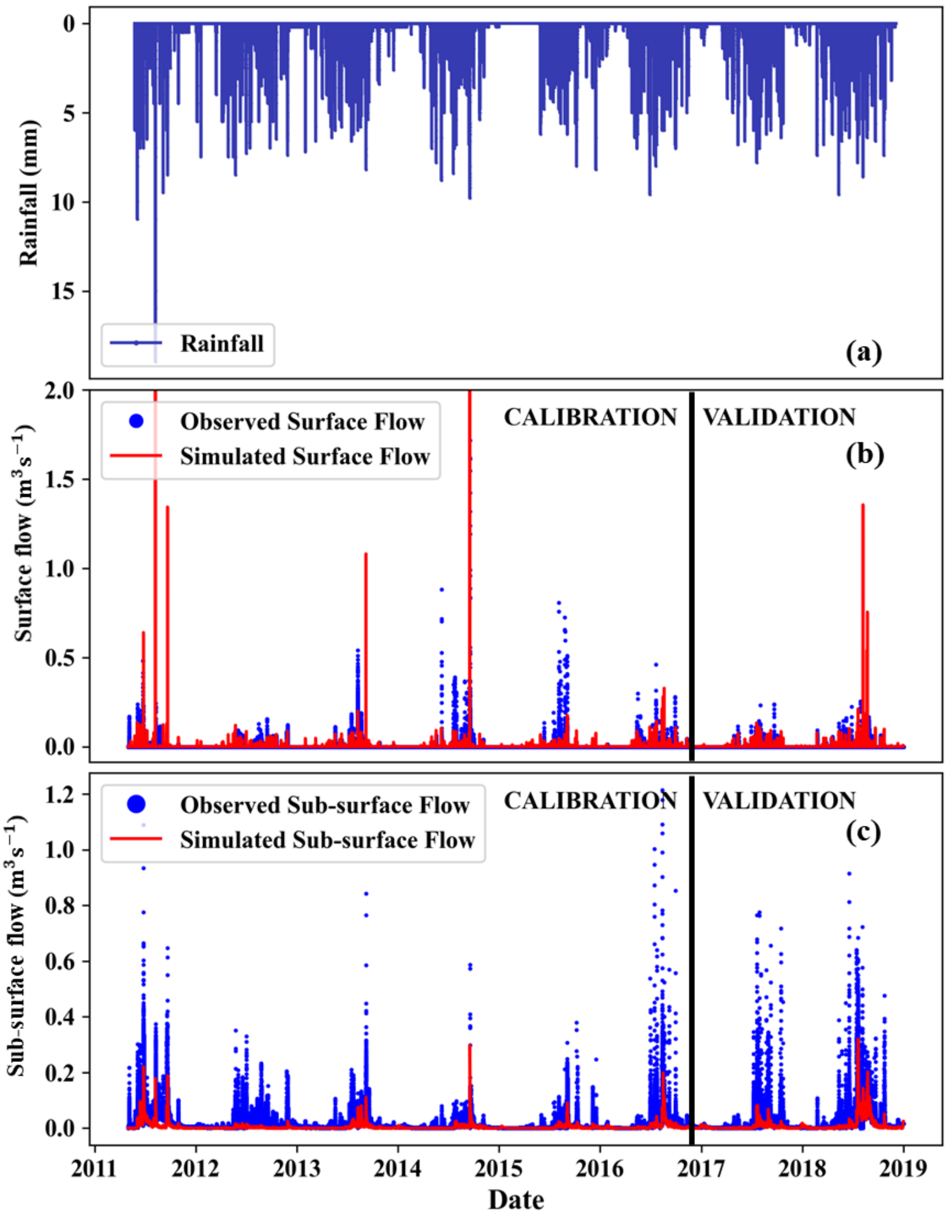

Figure 4: Hydrological simulation from HSPF: (a) Measured rainfall, (b) Simulated and observed surface flow, and (c) Simulated and observed sub-surface flow.

https://doi.org/10.5194/hess-2021-98
Preprint. Discussion started: 8 April 2021

Hydrology and Earth System Sciences
Open Access
EGU
Discussions

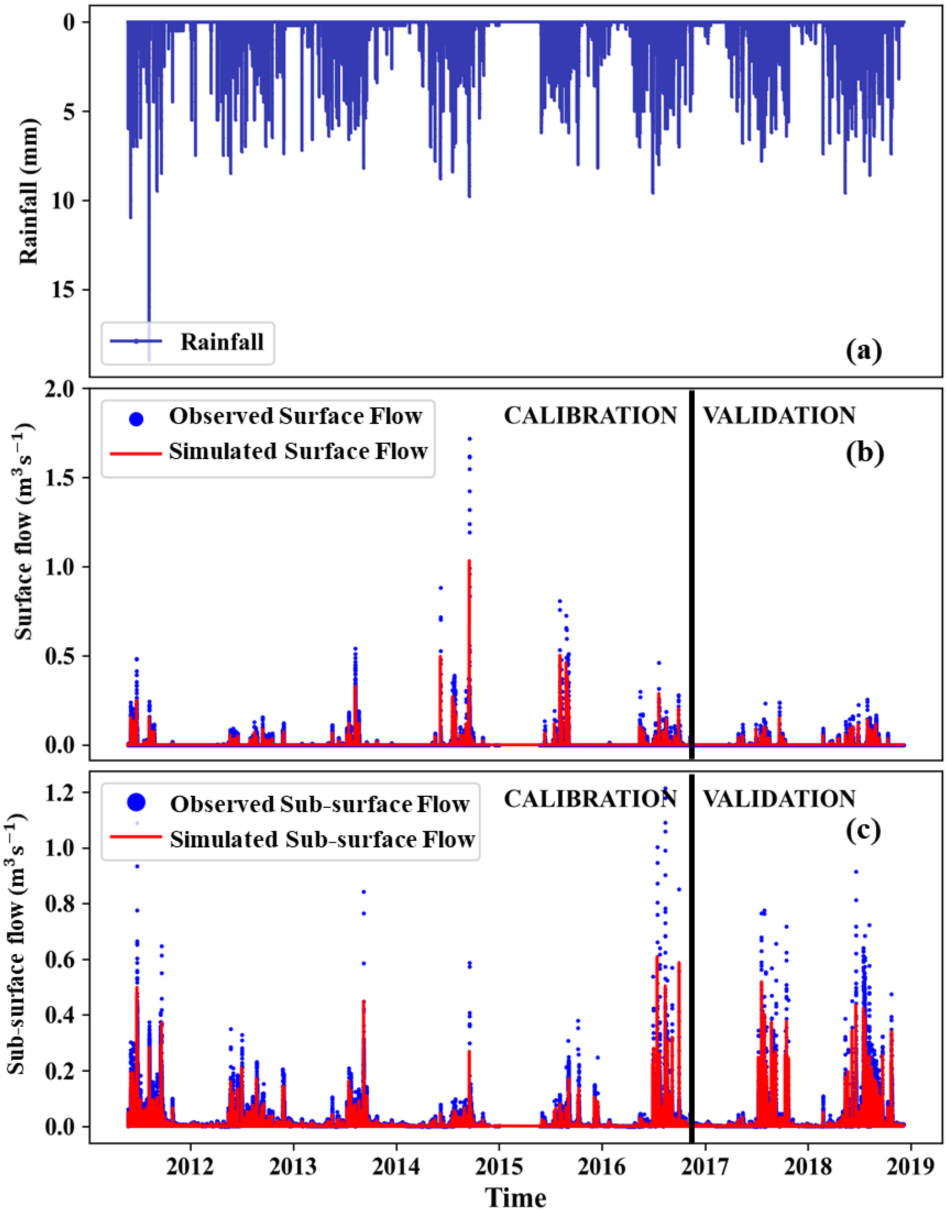

773

774 **Figure 5:** Hydrological simulation from LSTM: (a) Measured rainfall, (b) Simulated and
775 observed surface flow, and (c) Simulated and observed sub-surface flow.

Hydrology and Earth System Sciences
Discussions

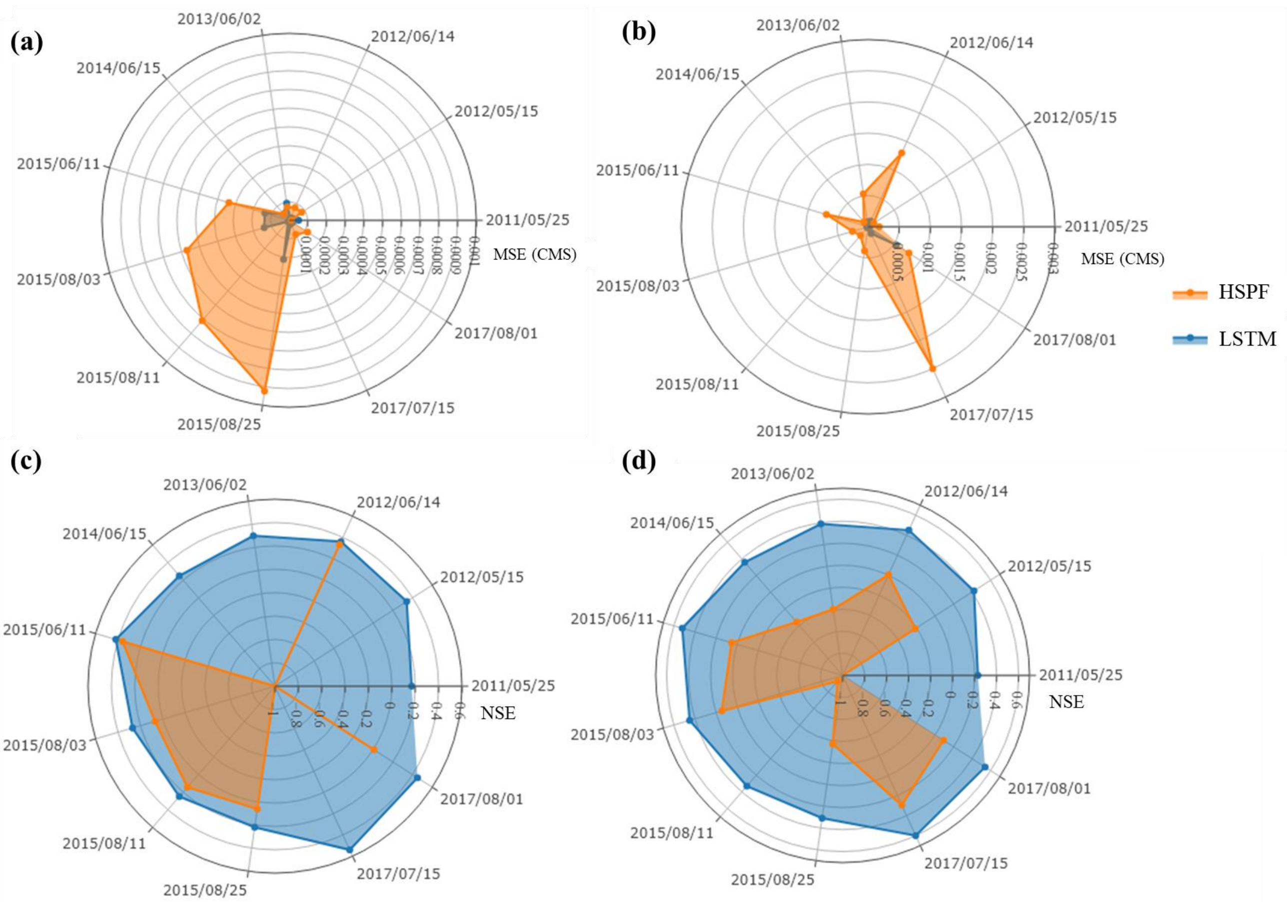

776

777 **Figure 6:** Comparison of the hydrological simulation during storm events: (a) MSE value of the
778 surface flow, (b) MSE value of the sub-surface flow, (c) NSE value of the surface flow and, (d)
779 NSE value of the sub-surface flow.

https://doi.org/10.5194/hess-2021-98
Preprint. Discussion started: 8 April 2021

Hydrology and Earth System Sciences
Discussions

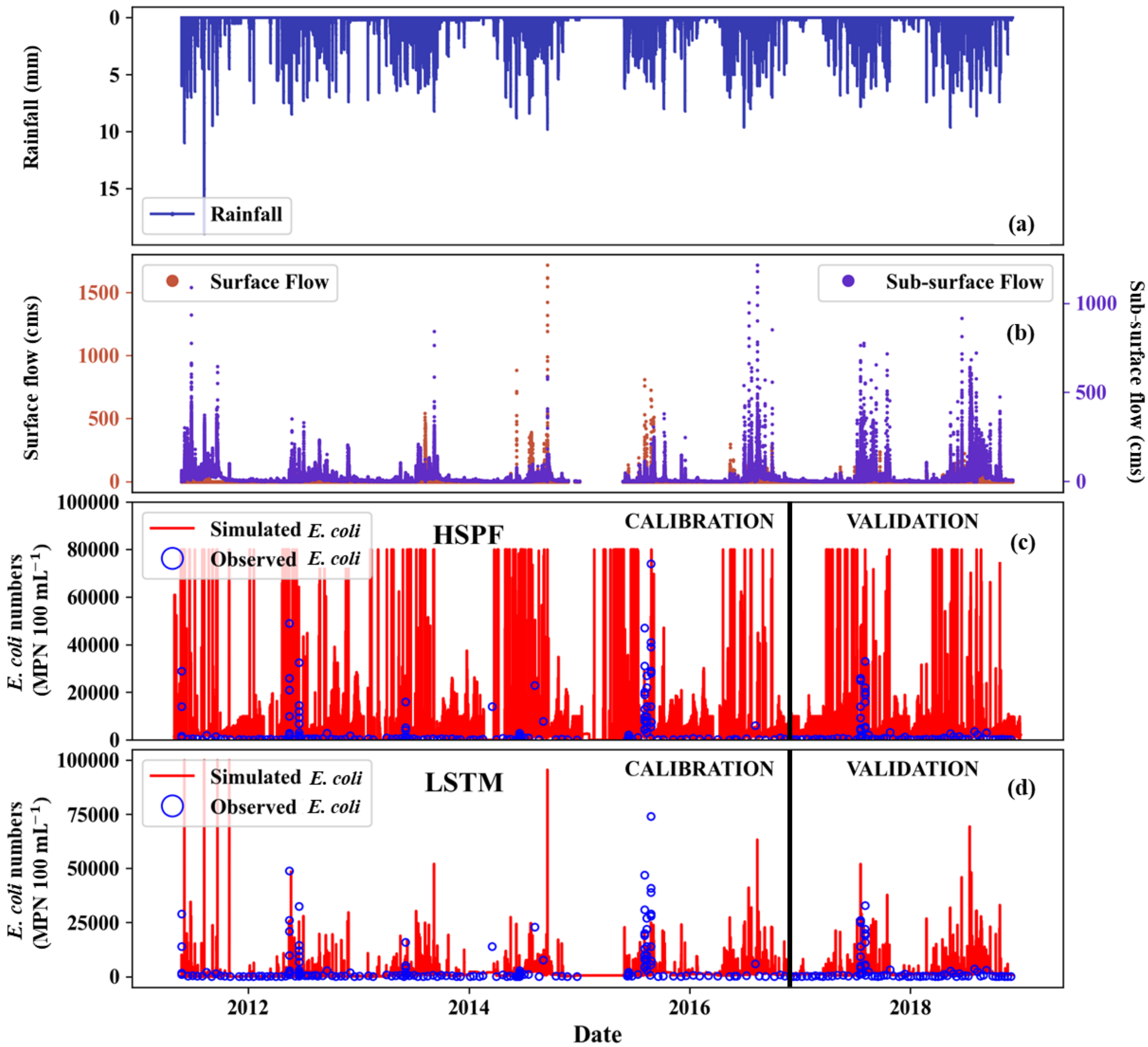

Figure 7: *E. coli* simulation from LSTM and HSPF: (a) Measured rainfall, (b) Observed surface and sub-surface flow, (c) Simulated and observed *E. coli* using HSPF, and (d) Simulated and observed *E. coli* using LSTM.

https://doi.org/10.5194/hess-2021-98
Preprint. Discussion started: 8 April 2021

Hydrology and Earth System Sciences
Open Access
Discussions

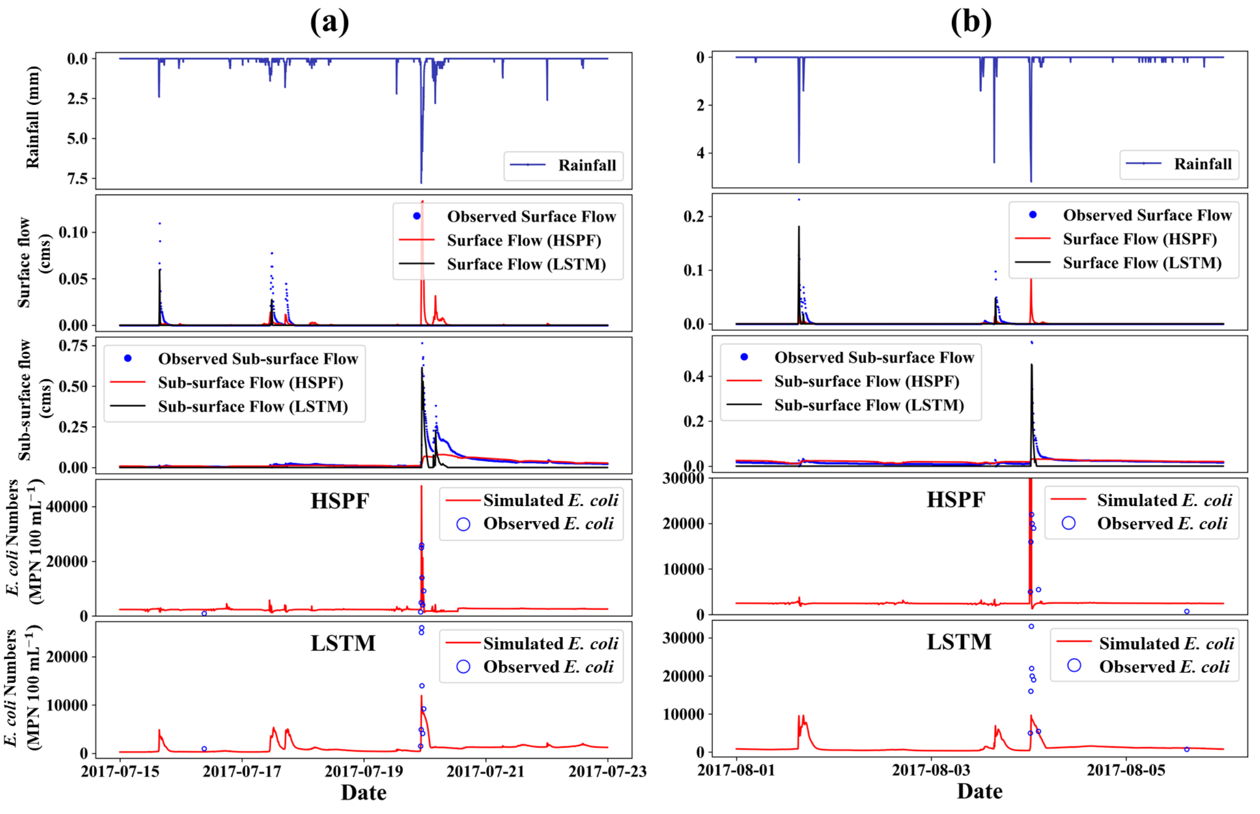

784 **Figure 8:** *E. coli* concentration of HSPF and LSTM on July 15 and August 1, 2017. Both storm

785 events were affiliated in validation period.

https://doi.org/10.5194/hess-2021-98
Preprint. Discussion started: 8 April 2021

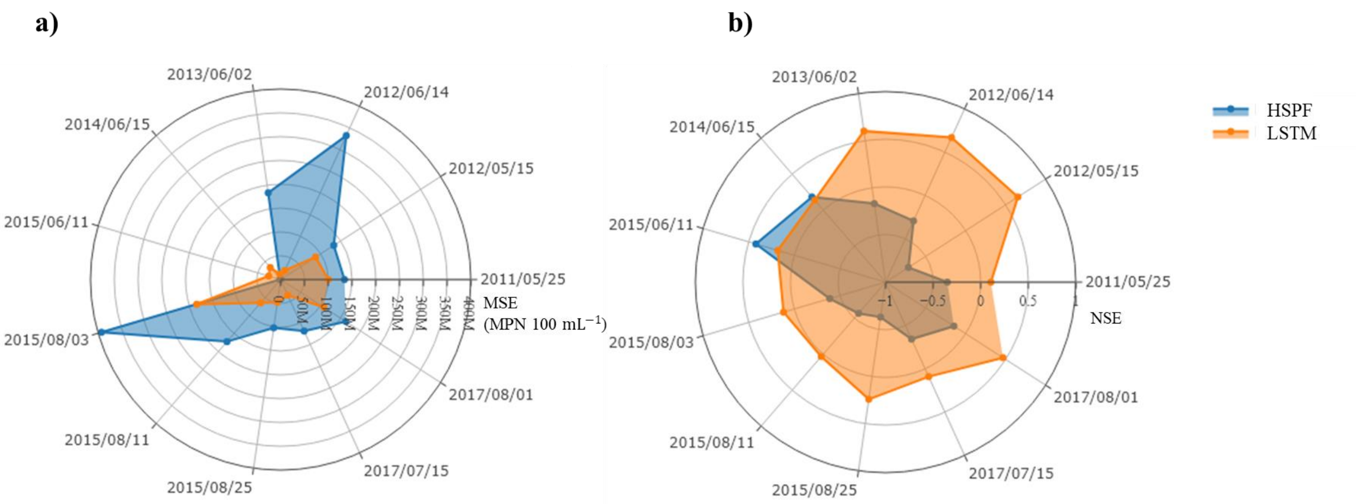

786

787 **Figure 9:** Comparison of the *E. coli* simulation during storm events: (a) MSE values and (b)

788 NSE values.

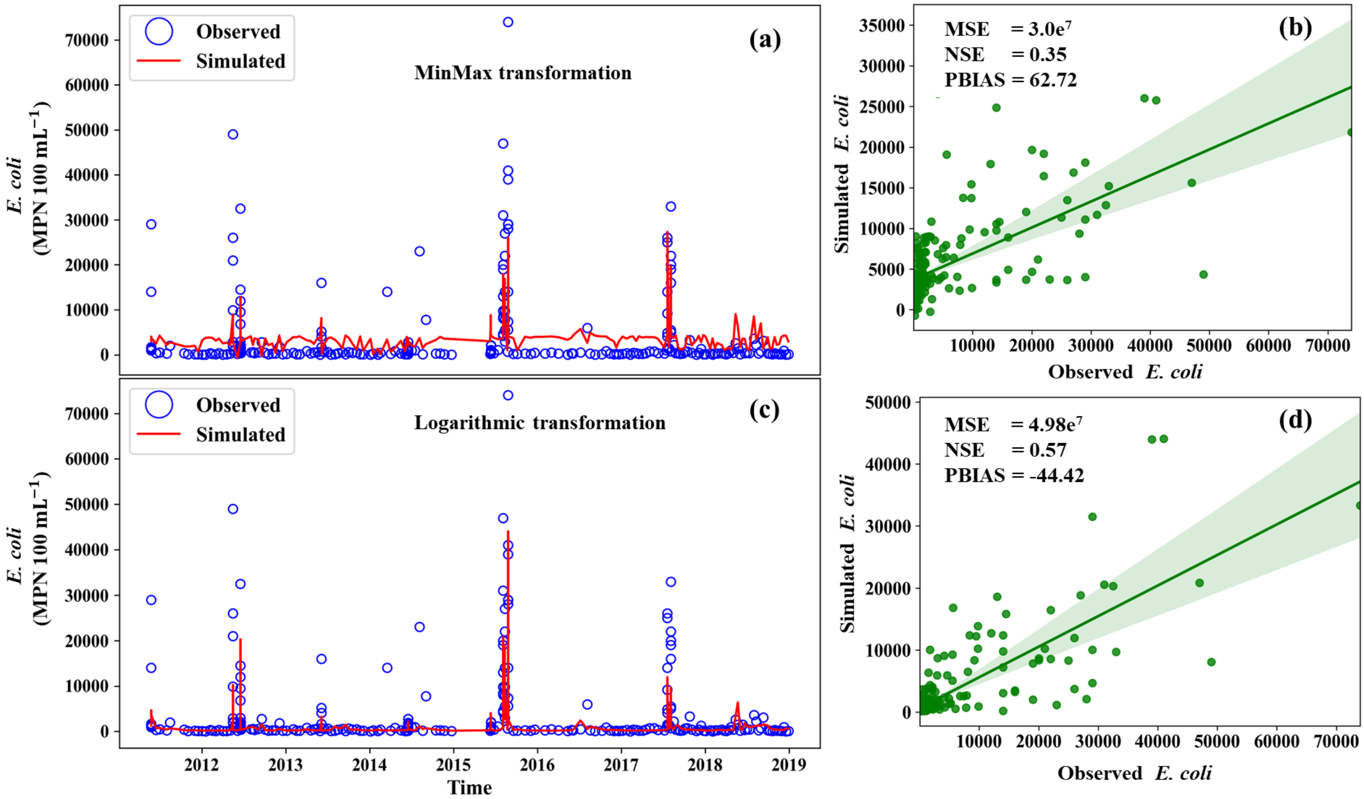

789 **Figure 10:** Comparison of *E. coil* concentration simulation with the transformation method: (a)
790 and (c) indicate the *E. coli* simulation using minmax transformation and logarithmic
791 transformation, respectively. (b) and (d) indicate the scatter plot of *E. coli* using minmax
792 transformation and logarithmic transformation, respectively.

https://doi.org/10.5194/hess-2021-98
Preprint. Discussion started: 8 April 2021

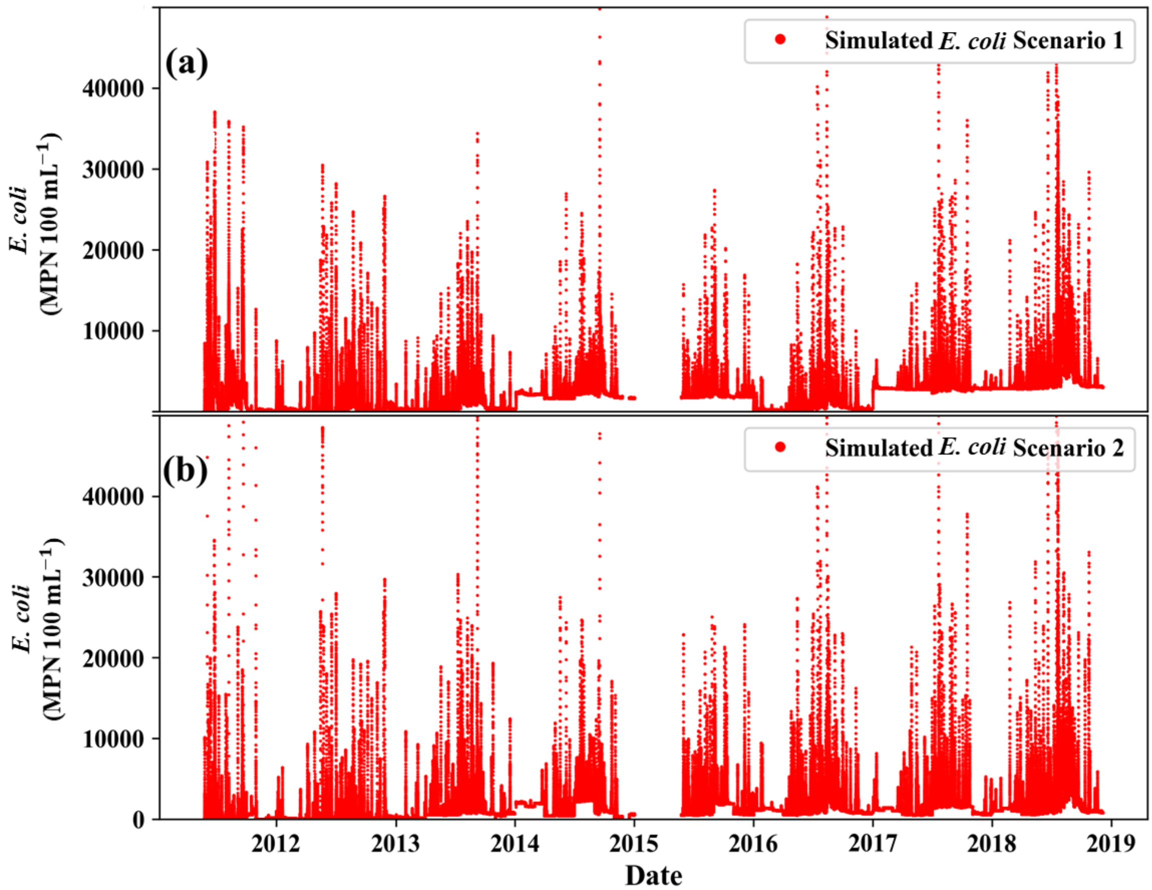

Figure 11: Changes in *E. coli* sources with land use change scenarios. Scenario 1 used land use change and bacterial source information. Scenarios 2 used the bacterial source by the fraction of each land use.